

ESTIMATING COVER AND MANAGEMENT FACTOR IN RUSLE BY NDVI TIME SERIES FOR ACROSS IRAQ-IRAN BORDER WATERSHED

Jumana Hadi Sahib^{1,2} and Ali H. Al Aboodi³

- ¹ PhD student at Department of Civil Engineering, College of Engineering, University of Basrah, Basrah, Iraq.
- ² Department of Civil Engineering, College of Engineering, University of Kufa, Kufa, Iraq. Email:jumanai.ALsabarawi@uokufaedu.iq.
- ³ Department of Civil Engineering, College of Engineering, University of Basrah, Basrah, Iraq. Email:ali.duhaim@uobasrah.edu.iq.

https://doi.org/10.30572/2018/KJE/160321

ABSTRACT

Land cover is essential for accurately observing land-use changes and assessing soil erosion risks. The study area between the Wasit, Misan, and Thi-Qar governorates is an ecological zone suffering from human-made soil erosion as crop cultivation, livestock grazing, etc. This research aims to analyze vegetation dynamics and evaluate soil cover utilizing Normalized Difference Vegetation Index (NDVI) data from 2013 and 2018-2021 during summer and winter, leveraging Landsat-8, Operational Land Imager (OLI) and a Thermal Infrared Sensor (TIRS), and QGIS. Warmer months exhibited a decrease in water bodies and vegetative cover compared to colder months. The changes from 2013 to 2021 were about 17%, distributionally as a 21% reduction in winter and 3.5% in summer. NDVI values and C-factor of RUSLE were calculated to estimate soil erosion, where Slight erosion occurrences exceeding 70%, while moderate and higher levels are found near Lake Shewicha and temporary water bodies. High to extremely high erosion types concentrated in tributaries of the Tigris River. Soil erosion increased between 2013 and 2021 by 4.2 and 18 Km2, respectively. The erosion soil for 2013 increased in November compared to April, except for slight to moderate and very high erosion, which decreased by 2%. In 2021, erosion decreased in December compared to April for all types, except for slight erosion increased by about 6%. The findings aim to help urban planners and land-use managers promote sustainable land management and soil conservation.



KEYWORDS

Land cover, NDVI, C-factor, RUSLE, GIS, Soil Erosion.

1. INTRODUCTION

As urbanization accelerates globally, effective land management strategies are crucial for addressing environmental challenges, particularly in rapidly developing regions (Morgan, 2005);(Salih & Dhiaa, 2023) like Iraq. Land use refers to how humans utilize specific areas for crop cultivation, livestock grazing, etc. In contrast, land cover describes the natural or humanmade elements, such as vegetation, on the land surface. It is greatly affected by drought, floods, burning, etc. (Durigon et al., 2014). To protect the soil from various climatic factors such as scarcity of water, cropping, livestock husbandry, urbanization, and agriculture are an insulating layer of the land cover (Al-Bahrani et al., 2021). Previous research has demonstrated that vegetation cover significantly reduces soil erosion by enhancing infiltration and minimizing surface runoff (Adekalu et al., 2006). Therefore, creating accurate maps of land cover is essential for effective management. Land cover maps are a tool for combating disasters, updating conservation strategies, addressing environmental disturbances, and combating erosion. Different vegetation types and human activities protect or expose the soil to erosive forces. If not managed sustainably, agricultural practices can lead to increased vulnerability and loss of topsoil. Additionally, urbanization often exacerbates erosion due to the removal of vegetation and the increase in impervious surfaces, which can cause higher runoff and sediment displacement.

So, the soil erosion models included the effect of vegetation cover and the land. The equation of soil erosion (USLE) and its revised equation (RUSLE) (Wischmeier & Smith, 1978; Renard et al., 1997); (Cheng et al., 2024) is considered one of the most famous equations for estimating soil erosion. It is expressed in terms of cover management and is symbolized by (C-factor). It is a link between soil erosion in areas with cover of vegetation and areas with tilled soils or soils that are permanently bare during cropping periods. To provide information on cover management, field surveys are used. Recently, new technologies have been relied upon to provide essential cover management, like remote sensing (Meusburger et al., 2010). This tool is essential for collecting surface data that facilitates vegetation mapping, is low-cost, fast, and accurate in analyzing data, and requires less equipment than on-site surveying. In addition, the data from remote sensing can be employed with GIS to facilitate the identification and assessment of soil erosion.

Identifying any changes in vegetation cover is a necessary step in understanding the system on Earth. There are several ways to identify changes in vegetation cover, where they are located, and how to measure them, such as the percentage of images, the difference in images, and others. Knowing the extent of vegetation growth through vegetation cover indices is one of the

most widely used (Richards, 2022), which depends on measuring specific types of radiation. (VIs) are calculated from the equation that primarily depends on the electromagnetic spectrum regions, which the near-infrared (NIR) and red (Tucker, 1979);(Nourizadeh et al., 2023). Biophysical data indicated spatial and temporal changes (Im et al., 2012). The soils with the highest electromagnetic radiation ratios are areas with sparse vegetation. As for the most negligible radiation, the soils with dense vegetation cover contribute to reducing radiation (Durigon et al., 2014). the vegetation cover evaluates the relationship between the vegetation and the erosion of the soil (Zhongming et al., 2010). It also depends on the location and density of trees and the density of branches and leaves

(Ichii, Kawabata and Yamaguchi, 2002) established climate parameters linked to the universal (NDVI). They demonstrated that temperature significantly affects biological activity, especially at high to mid-latitudes in the northern hemisphere, as temperature varies greatly between years. (Wang et al., 2003) indicated that vegetation production and, thus, NDVI are directly affected by rainfall. The relationship can be predicted by analyzing the appropriate spatial pattern. The factors that result the differences in the cover land and NDVIs are climate, relief, hydrology, and land use (Yun-hao et al., 2001);(Cheng et al., 2024).

NDVI measures vegetation activity, separating green vegetation from other surfaces, as chlorophyll needs red light for photosynthesis and reflecting near-infrared (NIR) wavelengths. The NDVI index has become helpful in analyzing satellite images to determine vegetation cover differences. Suppose the NDVI function is for two bands, both near-infrared and red spectrum (Defries & Townshend, 1994), (Garrigues et al., 2007); (Nourizadeh et al., 2023). The NDVI will calculate the vegetation cover for two dates separately. Then, the results of the two dates will be subtracted from each other, and the most recent date will be subtracted from the oldest. This will produce a layer containing the difference in vegetation cover during that period, which will be less affected by topography and lighting (Li et al., 2005), (Lu et al., 2005). This approach is called post-classification. This method makes it easy to obtain the variations in the vegetation cover in the study, and it also provides a study in which the spectral classifications of the images are compared. Draw maps of the type of natural transformation in the two dates (Singh, 1989);(Al-doski, 2013).

Despite numerous studies on land use and soil erosion, a notable lack of research focuses on the specific effects of climate factors like rainfall on vegetation cover in the Iraq-Iran border region. The study intended to assess changes in vegetation cover and analyze their relationship with soil erosion in a watershed between Kut and Amara, utilizing NDVI data from 2013 to 2021. By elucidating the dynamics of vegetation cover and its role in soil erosion, this research

aims to inform land management practices and enhance sustainability in the region.

2. STUDY AREA

The study area is between three governorates: Wasit, Misan, and Thi Qar, which are in the eastern part of Iraq and extend to the Iraqi-Iranian border, as shown in Fig.1, which extends from the highlands in Iran to the plains in central Iraq. Approximately seventy-five percent of the study area includes flat terrain, showing a mild gradient in the southwestern regions. The remaining twenty-five percent is in the northeastern regions and along the Iranian frontier. This region is observed by valleys interspersed with low anticlinal folds. The altitudinal difference in the study area is from 3 to 250 meters, with a mean elevation of 126.5 meters above the average mean sea level (Al-Abadi et al., 2016). It consists of three main basins, namely Lake Shuwaija, the Tigris River, and the AL-Teeb River, which were determined based on (DEM). Its raised temperatures and aridity describe this geographical area during the summer season, cold conditions in the winter, and temperate weather during the spring and autumn. Almost 90% of the yearly precipitation occurs from November and April, mainly during the winter months of December through March. The subsequent six months demonstrate conditions that are both dry and exceedingly warm. The region recorded an average annual precipitation of about 212 mm/year, considered by a varying distribution of rainfall between the plains and mountainous regions; furthermore, through the application of technologies remote sensing, the vegetative cover of this area will be quantitatively assessed (Al-Abadi et al., 2016).

3. DATA SET

The land use change raster data was sourced from the Landsat 8 satellite, launched on February 11, 2013, to monitor the Earth. This launch was part of the Landsat Data Continuity Mission (LDCM), a partnership between NASA and the U.S. Geological Survey (USGS). Landsat 8 is equipped with an Operational Land Imager (OLI) and a Thermal Infrared Sensor (TIRS), enabling the study of global warming by monitoring Earth's surface temperature. The data for this study, covering the years 2013 and 2018–2021, was obtained from the USGS website (https://earthexplorer.usgs.gov). While efforts were made to collect raw raster images for both summer and winter over these five years, some images were used due to cloud cover. Ultimately, two images per season were downloaded each year, resulting in a total of 20 images to cover the study area.

4. METHOD

The combination of the (GIS) and Remote Sensing methodologies enhanced the accuracy of estimates of the RUSLE model, which was primarily developed by (Kebede et al., 2021) (Fenjiro et al., 2020). The RUSLE model was affected by some factors: cover the land (c), soil

(K), terrain (LS), rainfall (R), and practice of support (P). This model was utilized to evaluate the spatial distribution of soil erosion by the following equation:

$$A = R \times K \times LS \times C \times P \tag{1}$$

where A represents the mean loss of soil (t /ha*year), R denotes the erosivity of rainfall (MJ mm/ ha*h* year), K indicates soil erodibility (t /ha*MJ* mm), LS refers to topographic factor, C signifies the vegetation cover, and P corresponds to control practice.

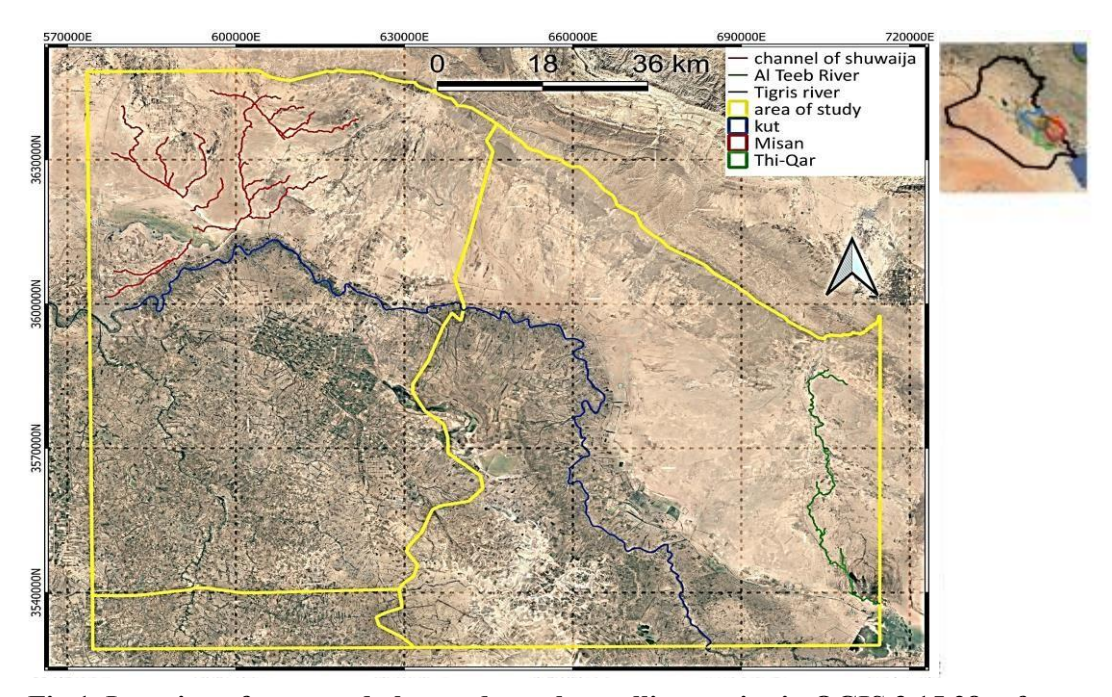


Fig.1. Location of area study by used google satellite service in QGIS 3.15.28 software

4.1. THE EROSIVITY OF RAINFALL

The factor of rainfall erosivity (R) is a key driver of rain-induced erosion. It reflects the impact of rainfall and subsequent runoff on the soil surface in a specific geographic area. It is widely recognized in the literature as a fundamental factor in soil erosion processes (Abdulkareem et al., 2017). This study collected detailed rainfall data from 2003 to 2021 from the Bureau of Meteorology. This data was processed using QGIS software version 3.15.28, utilizing the kriging method for interpolation. The R-factor was then estimated using the equations below and applied to the (RUSLE) model.

$$R = 587.8 - 1.219p + 0.004105p^2 \quad p \ge 850 \tag{2}$$

$$R = 0.04830p^{1.6} p < 850 (3)$$

mean annual rainfall (p)mm.

4.2. ERODIBILITY OF THE SOIL

Soil erodibility, denoted as the K factor, indicates the soil's long-term response to erosive forces, which are influenced by rainfall dynamics and subsequent runoff (Abdulkareem et al.,

2017). To determine soil type, soil samples were obtained from the field and classified using sieve analysis. The K factor was computed using equations (4) and (5), with interpolation performed through the kriging method using QGIS 3.15.28 software.

$$K = 7.594 \left\{ 0.0017 + 0.0494 \exp \left[-\frac{1}{2} \left(\frac{\log (Dg^2) + 1.675}{0.6986} \right)^2 \right] \right\}$$

$$Dg(mm) = \exp \left(0.01 \sum_i f_i \ln m_i \right)$$
(5)

Here, f represents the primary particle size fraction in percentage, while m denotes the arithmetic mean of the particle size boundaries of that fraction.

4.3. TERRAIN FACTOR

The terrain factor, represented by the LS factor, explanations the impact of geomorphological processes on erosion, incorporating both slope length and steepness (Lü et al., 2012);(Cheng et al., 2024). To calculate the LS factor, raster data from a Digital Elevation Model (DEM) created from topographic maps was used. The LS factor was computed using QGIS 3.15.28's raster calculator module, applying the following equation:

$$LS = \left(\frac{A_5}{22.13}\right)^m \left(\frac{\sin\theta}{0.0896}\right)^n \tag{6}$$

where the slope length represents as θ denotes the slope angle, m indicates the variable slope length power, and n signifies the slope steepness power.

4.4. THE PRACTICE CONTROL FACTOR

The practice control factor, or support practice factor in the RUSLE equation, is a dimensionless ratio that compares soil loss under specific management practices to tilled soil. These practices aim to reduce runoff by altering slope steepness, flow patterns, or direction (Gong et al., 2022). The factor varies from 0 to 1, where reduced values signify enhanced runoff control. In this study, approximately 92% of the area is bare soil, so the P factor was set to 1 for the RUSLE model soil erosion estimation.

4.5. THE VEGETATION COVER FACTOR

The vegetation cover factor, or C-factor, quantifies vegetation's protection against rainfall-induced erosion in the RUSLE (Wischmeier & Smith, 1978);(Renard et al., 1997);(Xiong et al., 2023). It denoted the link between soil degradation, certain vegetation cover, and management practices compared to bare, tilled soil. Estimating the C-factor using the (NDVI) from high-resolution images yields more accurate results than traditional methods without NDVI (Vatandaşlar & Yavuz, 2017). The equations developed by (Knijff et al., 2002) can be effectively applied to the highland regions of northeastern Iraq and other vulnerable ecosystems (Nourizadeh et al., 2023). The quantity, type, and growth stage of vegetation significantly

influence the C-factor, as vegetation mitigates rainfall's kinetic energy before soil impact, reducing erosion (Qian et al., 2022). In this study, the C-factor was estimated using the rescaled NDVI (Tucker, 1979)(Nourizadeh et al., 2023) as follows:

$$NDVI = \frac{\rho NIR - \rho \operatorname{Red}}{\rho NIR + \rho \operatorname{Red}}$$
(7)

$$NDVI = \frac{\text{band } 5 - \text{band } 4}{\text{band } 5 + \text{band } 4} \tag{8}$$

$$C \text{ factor } = e^{\left(-2*\frac{NDVI}{1-NDVI}\right)} \tag{9}$$

The C-factor can be mapped using remote sensing to create a spatial model for improving soil erosion assessment (Meusburger et al., 2010). Remote sensing deals with several benefits over traditional data collection methods, such as the ability to use GIS to detect differences in land use (Weng, 2002; Oñate-Valdivieso & Sendra, 2010; Wu et al., 2006), assess soil degradation (El Baroudy, 2011), and evaluate soil erosion (Panagosa et al., 2015).

A difference in NDVI (DNDVI) was calculated to analyze vegetation changes. This process compares NDVI values from two different dates, using images where NDVI values range from -1 to +1 (Sellers, 1985; Spanner et al., 1990; Al-doski, 2013). The DNDVI image is created by subtracting the NDVI image from one date from that of another date (Cakir et al., 2006; Al-doski, 2013). In this study, the NDVI image from 2013 was subtracted from the 2021 image using the equation below:

$$DNDVI = NDVI (2013) - NDVI (2021)$$
 (10)

As noted, changes in the C-factor are critical for calculating soil erosion in various regions, making it essential for sustainable soil erosion management. To create a C-factor map, temporal images from the OLI sensor on the Landsat 8 satellite, (the USGS website (https://earthexplorer.usgs.gov)), were used from 2013 and 2018 to 2021. The visible and near-infrared bands have a spatial resolution of 30 x 30 meters. The C-factor was calculated twice for 2013 and 2018–2021. Using Eq.8, the NDVI was derived from these images, and the C-factor was calculated using Eq.9 within the QGIS 3.15.28 software.

5. THE RESULT

The RUSLE model factors were estimated utilizing (GIS) technology to consider all the various factors. It was used in the years 2013 and 2018 to 2021 by Eq.1. The spatial resolution was 30 meters. The result of these factors P, R, K, C, and LS are displayed in Fig.2.

5.1. The Vegetation Cover Factor

After downloading the raw images into QGIS 3.15.28 software, several images contained cloud

cover, obscuring the true reflection of the vegetation. These clouded images were excluded from the analysis. For 2013, 2018, and 2021, NDVI values were calculated twice yearly—once in summer and once in winter. Water bodies and vegetation tend to decrease in warmer months, while colder months show more abundant vegetation. This seasonal difference resulted in variations in C-factor values, as changes directly influence them in the vegetation index (Nourizadeh et al., 2023).

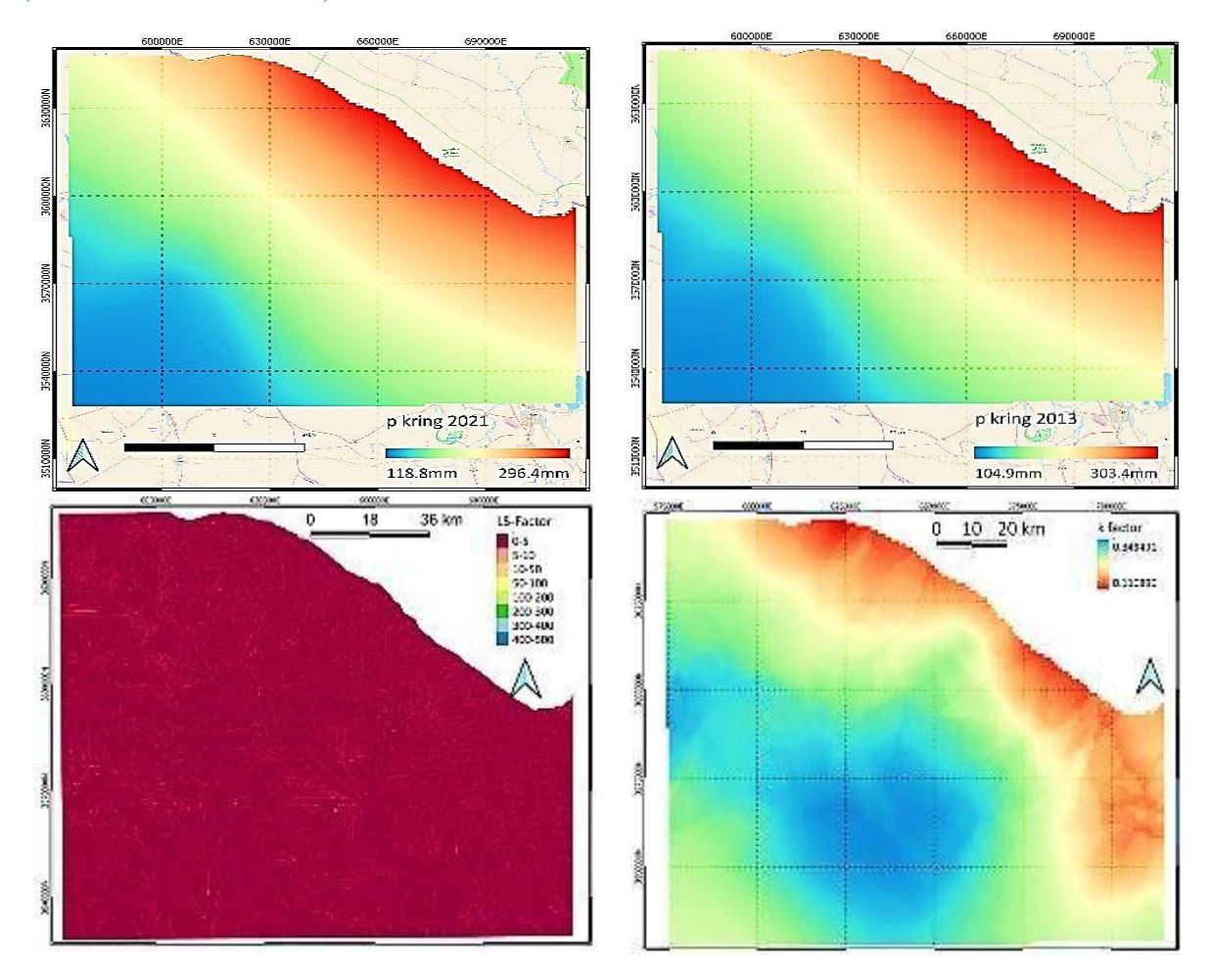


Fig.2. The result of R factor 2013 and 2021, LS factor, K factor by QGIS 3.15.28 software

In the study area, the cover of vegetation results indicated that the landscape mainly consists of water bodies, bare soil, sparse vegetation, and a few regions with medium-density plant cover. Overall, the area has little vegetation. The NDVI values, crucial for evaluating vegetation health and coverage, were accurately calculated using satellite data from Landsat 8, (the USGS website (https://earthexplorer.usgs.gov)), covering 2013 and 2018- 2021. These values ranged from -1 to +1 (Al-doski, 2013). Negative NDVI values correspond to surface types such as water bodies, clouds, and snow, while values around zero represent bare soil or rock. Healthy, green vegetation typically shows NDVI values close to +1, reflecting strong photosynthetic

activity and vitality. NDVI values below 0.2 indicate either water bodies or an absence of vegetation. Sparse vegetation is represented by values from 0.2 to 0.4, moderate vegetation cover between 0.4 and 0.6, and dense vegetation cover by values above 0.6.

In this study area, the vegetation cover results show that the area consists of bodies of water or soil without vegetation cover, sparse vegetation, and few areas containing plants of medium density. There is little vegetation cover.

After processing the satellite images, those affected by cloud cover were removed from the analysis for 2013 and 2018-2021. As a result, different months were selected for evaluation. For example, the fourth month was chosen to represent winter (the end of summer), while months 10, 12, and 11 were selected for 2018, 2013, 2020, 2019, and 2021, respectively, ensuring cloud-free images were used.

NDVI was calculated for both summer and winter across 2013, 2018, and 2021, focusing on cloudless days and aiming to capture data at the end of each seasonal period whenever possible, as shown in Fig.3. These calculations revealed a significant gap in vegetation cover between summer and winter. Warmer months saw reduced water bodies and less vegetation, resulting in lower NDVI values, while colder months displayed more vegetation, leading to higher NDVI values. In some years, particularly in 2018, vegetation almost entirely disappeared by the end of the summer due to extreme temperatures. This left minimal plant life, whereas sparse vegetation was observed during winter. Notably, 2018 exhibited minimal vegetation cover, even in winter, due to changing climate conditions.

These findings have profound implications for soil erosion. In hot summer months, when vegetation is scarce, the soil remains dry and loose, making it highly susceptible to erosion. When precipitation occurs in winter, the lack of vegetation to stabilize the soil increases erosion. Consequently, higher C-factor values are anticipated due to the NDVI calculations.

After a thorough differential analysis of the NDVI results between 2013 and 2021 for winter and summer, notable disparities in vegetated regions were observed and those lacking vegetation are evident, as shown in Fig. 4. The variations within the geographic region suggest that climate change plays a significant role, highlighting the diverse environmental impacts affecting the area. In the DNDVI image Fig. 4, regions with notable changes are marked in red and blue. Red indicates areas that have experienced a significant loss of vegetation, while blue represents areas where vegetation has increased. Regions with little to no change are shaded in neutral gray, offering a clear visual distinction of vegetation stability.

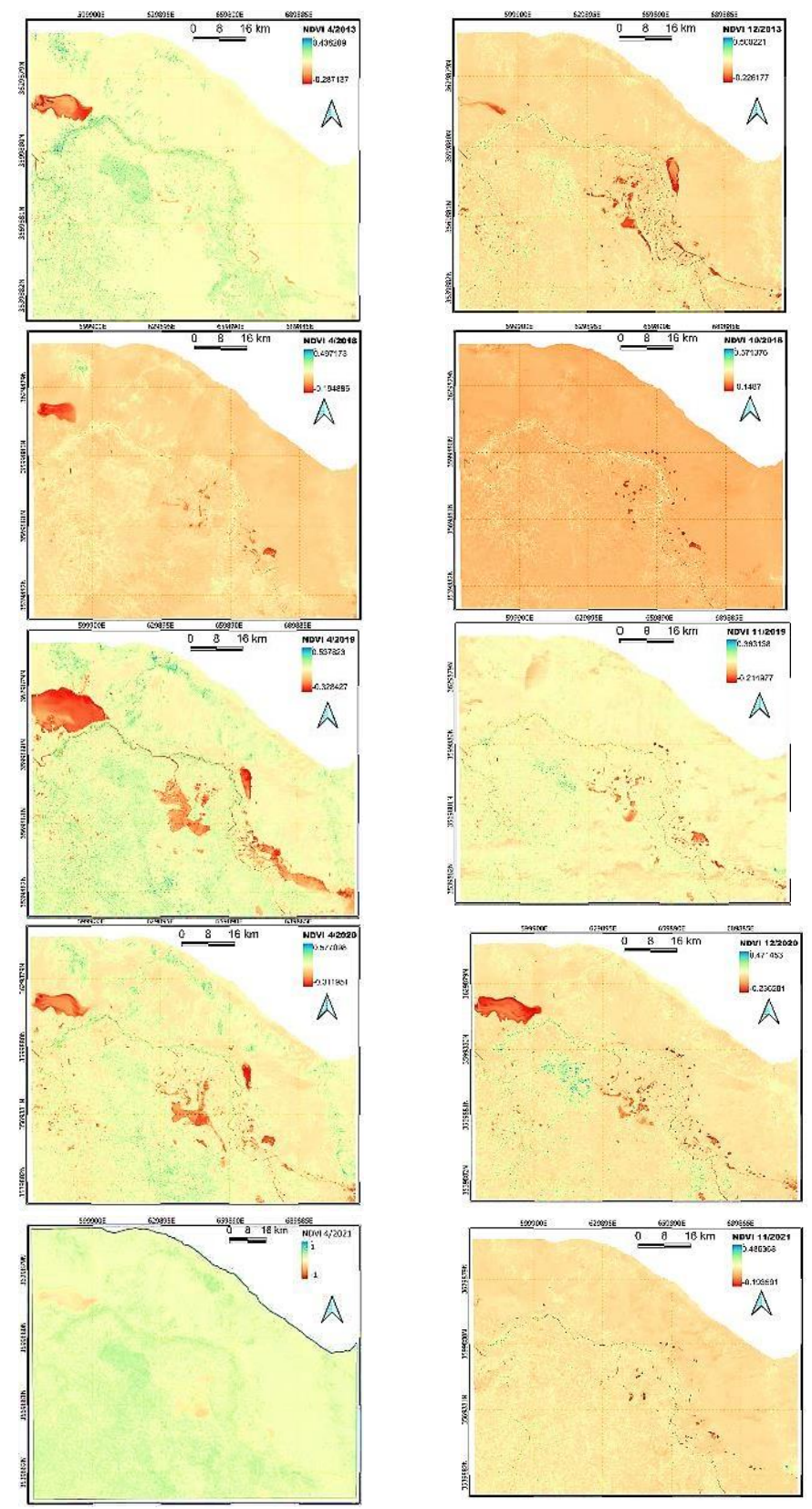


Fig.3. The result of NDVI for the winter and summer seasons by QGIS 3.15.28 software

The areas with the most substantial negative changes in NDVI values, indicating a decline in vegetation cover, are predominantly concentrated in agricultural zones. There was a significant seasonal difference in NDVI values between winter and summer. Between 2013 and 2021,

approximately 21% of the land exhibited reduced vegetation cover during winter, compared to about 3.5% during summer. The total change in vegetation cover between these two years, (2013 and 2021), amounted to around 17%, as outlined in Table 1.

As shown in Table 2, the most affected region within the study area is Thi-Qar Governorate, despite its relatively small size. It is followed by Wasit Governorate, with Misan Governorate experiencing the least impact.

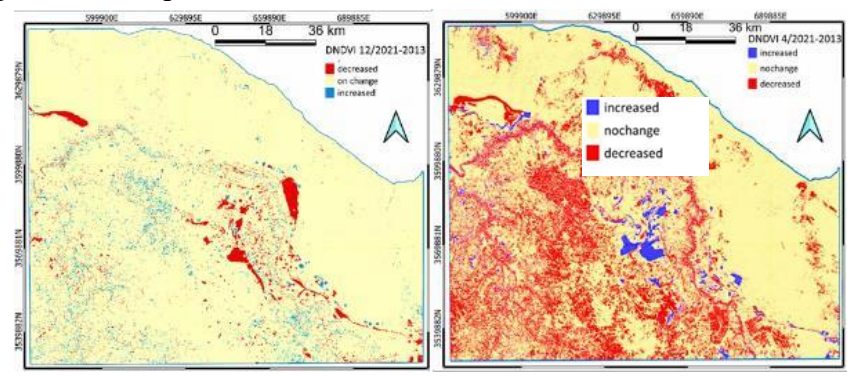


Fig.4. The difference between NDVI between 2013 and 2021 by QGIS 3.15.28 software

	total area	11/2	021-2013	4/2021-2013			
class	(Km2)	area class (Km2)	percentage area class	area class (Km2)	percentage area class		
increased	14221.17	351.391	2.470901	866.249	6.091264		
decreased	14221.17 14221.17	492.171 13377.57	3.460833 94.06801	3089.03 10265.94	21.72135 72.18772		

Table 1: the percentage area for changing in study area

Table 2: the percentage area for changing over government in study area

			DNDVI 4	4/2021-2013	DNDVI 12/2021-2013			
classes	government	Area (Km ²)	area class (Km ²)	%area	area class (Km ²)	%area		
increased		632.164	38.5	6.090192	34.652	5.481489		
decreased	Thi-Qar	632.164	239.51	37.88732	15.122	2.392101		
no change		632.164	354.15	56.02186	582.372	92.12356		
increased		6935.482	434.11	6.259262	191.3	2.75828		
decreased	Wasit	6935.482	1740.617	25.09728	144.7	2.086373		
no change		6935.482	4760.75	68.64339	6599.463	95.15507		
increased		6653.522	403.428	6.063375	126.8136	1.905962		
decreased	Misan	6653.522	1089.755	16.37862	333.377	5.010534		
no change		6653.522	5160.338	77.55799	6193.327	93.08344		

The appearance of C factor values is attributable to the varied vegetation indicators analyzed during the study. Upon showing a thorough investigation of the results about the coverage of vegetation, it became increasingly seeming that the geographical area under investigation was mainly categorized by the presence of wide water bodies, regions of soil that were conspicuously devoid of any significant vegetation, as well as isolated covers of sparse plant growth, alongside a limited number of zones that exhibited moderately dense vegetation, as shown in Fig.5.

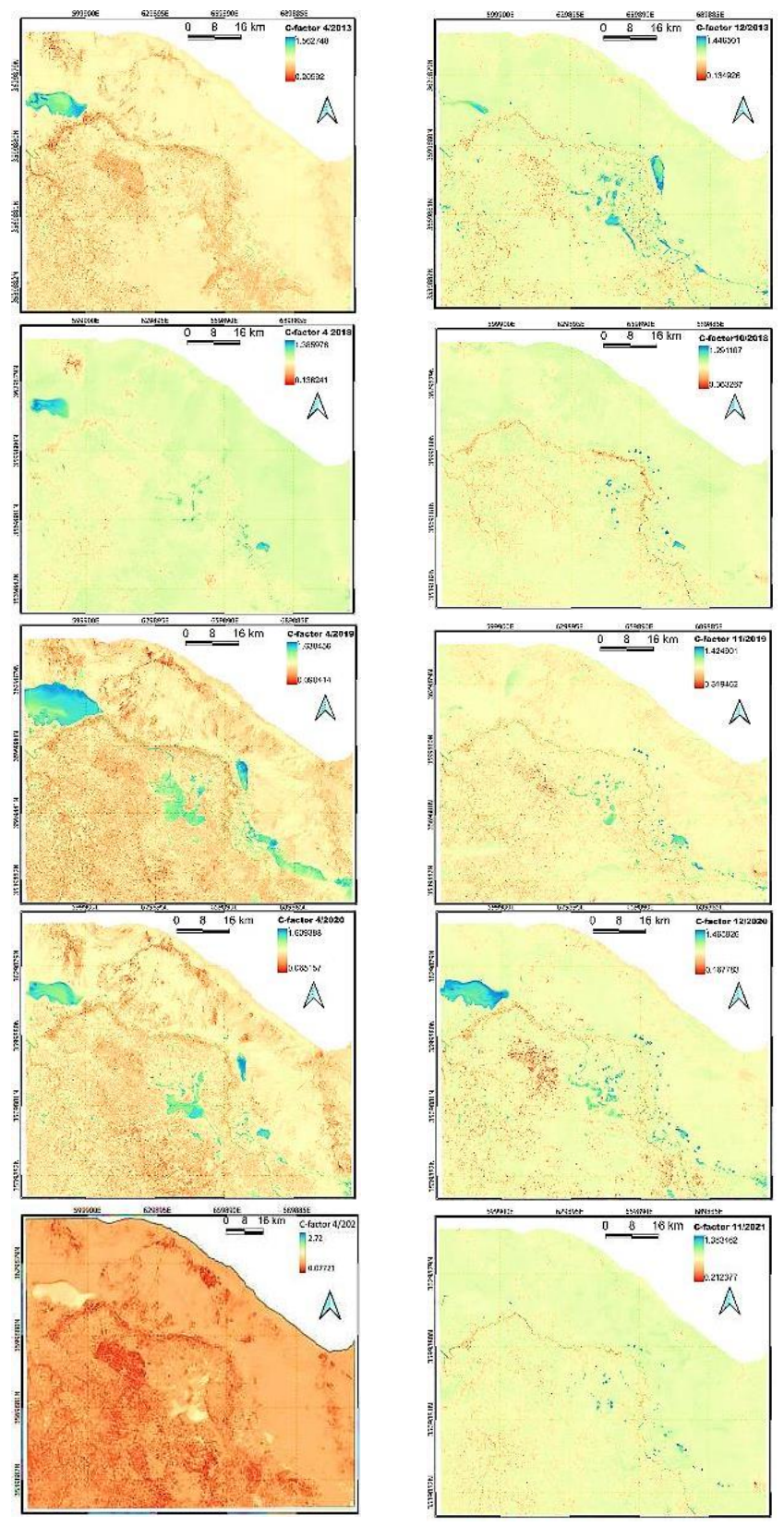


Fig. 5. The map of C- factor for area study by QGIS 3.15.28 software

5.2. The Result of Soil Erosion

Within the specified study region, the soil erosion intensity confronted has been analytically considered into levels: slight, sight to moderate, moderate, moderate to high, high, very high,

extremely high and extremely. Concurrently, a widespread erosion of soil map indicating spatial distribution for soil erosion through area study was skillfully created by QGIS version 3.28.15. After collecting data to calculate soil erosion factors using Eq.1, the effect of these factor layers was analyzed to estimate soil erosion for 2013 and 2021, as shown in Fig.6.

The control of slight erosion is in the general study area. In contrast, slight to moderate, moderate, and moderate to high in large parts of the total area are concentrated around water collection areas in Lake Shewicha and other temporary lakes. It is also apparent in the part of the upper catchment of the Teeb River and the small order around the Tigris River catchment. At the same time, the remains of the types are concentrated in the tributaries until extremely high erosion values are found in the body of the Tigris River. The control of slight erosion was observed throughout the study area, as its percentage ranged between more than 70% of the total area during the winter and summer seasons for the three governorates. This percentage reached 95% in the Dhi Qar Governorate and decreased to about 70% in the Misan Governorate, as shown in Table 3. In general, an increase in slight erosion is expected in 2021, with an estimated area of about 253 square kilometers at the end of winter and a decrease estimated at 168 square kilometers at the end of summer.

The types of soil erosion, sight to moderate, moderate, and moderate to high, it generally decreased between the end of winter and summer between 2013 and 2021, estimated at 146.77 and 63 and 11 square kilometers, respectively, for April. As for the erosion values at the end of summer, they increased for the slight to moderate and moderate types by about 187 and 3.5 square kilometers, respectively, while the moderate to high type decreased by about 8 square kilometers. As for the remains of the erosion types, they decreased between 2013 and 2021, as shown in Table 3. Generally, soil erosion increased between 2013 and 2021 by 4.2 and 18 square kilometers, respectively.

While the erosion values for 2013 increased in November compared to April, except for slight to moderate and very high erosion, which decreased by a high percentage of 2%, in 2021, erosion decreased in December compared to April for all types, except for slight erosion, it increased by about 6%.

From the above results, the decrease in slight erosion has been transformed into the rest of the types of erosion, indicating the lack of sufficient vegetation cover to reduce the effects of erosion. In addition, if no measures are taken to prevent increased erosion or mitigate its impact on erosion. It deserves urgent attention and should be prioritized to implement effective soil conservation measures to reverse these harmful trends.

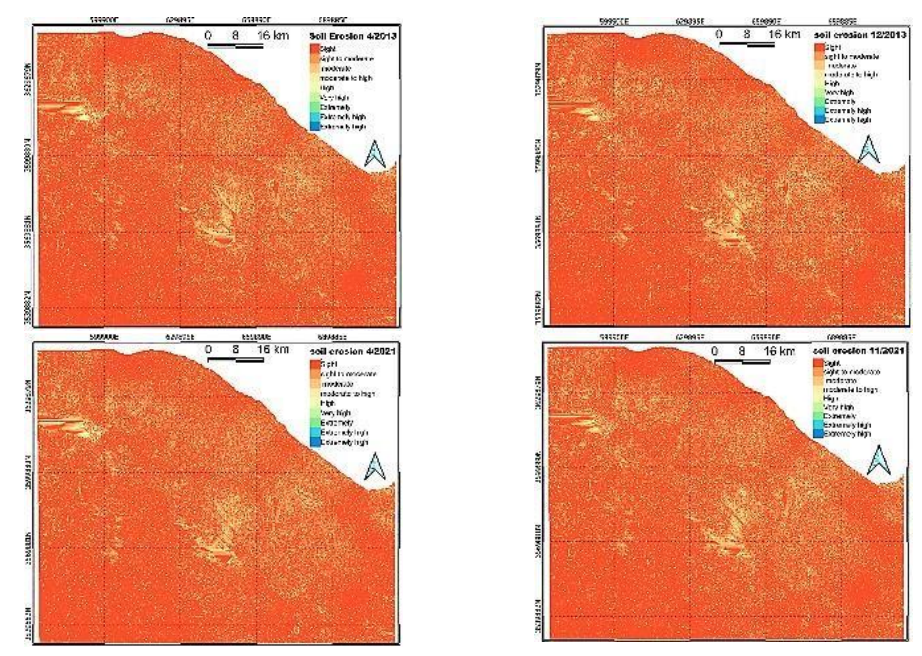


Fig.6. The map of soil erosion for area study by QGIS 3.15.28 software

6. CONCLUSION

This study employed the (NDVI) from high-resolution Landsat 8 imagery to determine the soil cover management (C-factor) within the (RUSLE) framework, focusing on a watershed in the study area. By combining remote sensing technology with GIS, the research provided an efficient method for analyzing spatial and temporal variability in soil cover. The NDVI analysis conducted for summer and winter from 2013 and 2018 to 2021 highlighted significant seasonal differences in vegetation cover. The warmer months exhibited a notable reduction in vegetation and water bodies, with around 21% of land showing decreased cover in winter compared to 3.5% in summer. Thi-Qar Governorate was the most affected area, followed by Wasit and Misan. The study found that slight erosion accounted for over 70% of the region, with more severe erosion concentrated around Lake Shewicha and the upper catchment of the Teeb River. Erosion types increased between 2013 and 2021, shifting from slight erosion to more severe types, indicating inadequate vegetation cover to mitigate erosion. The C-factor maps generated are valuable for emergency managers in assessing natural hazards and promoting urban sustainability. However, further validation and adjustments are needed to confirm their applicability in different topographies, vegetation types, and soil conditions.

Table 3: The %area Soil Erosion in the governments in 2013 and 2021

The result for 4/2013 and 2021

differe	ence en 4/ 2021	Ap20r-21							Apr-2013							
and 20		T	hi Qar	N	Iisan		Kut	Tl	hi Qar		Misan		Kut			
	A		%	A	%	A	%	A	%	A		%	%	A	%	
Sight 5351.			77.	re 4732.	71.	601.	95.	re 5492.	79.	re 4839	Are 7	2.74	96.	253.1	4	
-2.56	-146.77	2.21	13.97	13.39	891.09	10.50	728.41	2.66	16.79	14.43	959.80	11.59	803.6	5	Sight to Modera	
62.92	1.01	6.37	7.38	490.82	5.53	383.45	1,22	7.73	7.78	517.94	6.03	417.89	Moderat			
-0.22	-11.19	0.31	1.96	2.33	155.20	1.77	122.49	0.37	2.34	2.35	156.57	1.90	131.9	2	Moderate to high	
-8.66	0.15	0.92	1.08	71.87	0.83	57.73	0.17	1.05	1.10	73.31	0.93	64.81	Hig -0.1			
-0.27	-14.08	0.25	1.55	1.81	120.44	1.35	93.61	0.31	1.97	1.87	124.69	1.49	103.0)2	very high	
-0.07	-4.02	0.04	0.24	0.57	37.72	0.40	27.81	0.05	0.32	0.59	39.04	0.44	30.4	3	Extremely	
-0.03	-1.79	0.00	0.03	0.38	25.28	0.25	17.65	0.01	0.04	0.38	25.44	0.28	19.2	7	Extremely High	
-1.66	0.00	0.00	0.03	2.22	0.01	1.03	0.00	0.00	0.05	3.58	0.02	1.33 -0.02		-	g	

	erence veen 11-			Nov-	-2021				Classes					
12/2021 and 2013		Thi Qar Misan				K	ut	Thi (Thi Qar		Misan		Kut	
Area (K <u>m²)</u>		% area	Area (Km²)	% area	Are (Kn		Area (Km²)	% area	Ar (Kr		Area (Km²)	% area	Area (Km²)	% area
-2.87	-168.26	95.00	600.56	70.10	4664.1	76.49	5304.73	95.43	603.29	71.38	4749.16	77.65	5385.24	Sight
3.19	187.20	2.74	17.34	14.86	988.40	12.20	846.16	2.27	14.34	13.39	890.92	10.95	759.44	Sight to Moderate
3.55	1.26	7.94	8.11	539.46	6.20	430.32	1.21	7.68	8.12	540.39	6.14	426.10	Moderate 0.09	
-0.11	-8.30	0.40	2.54	2.46	163.95	1.89	131.42	0.39	2.45	2.54	168.81	1.95	134.94	Moderate to high
-4.91	0.17	1.09	1.16	77.22	0.89	61.51	0.17	1.09	1.18	78.68	0.94	64.97	High -0.07	
-0.06	-4.46	0.33	2.06	1.96	130.23	1.45	100.33	0.32	2.01	2.00	133.02	1.47	102.05	very high
-0.02	-1.23	0.05	0.34	0.61	40.45	0.43	30.16	0.06	0.37	0.62	41.21	0.44	30.60	Extremely
-0.02	-1.00	0.01	0.04	0.40	26.54	0.28	19.40	0.01	0.04	0.41	27.11	0.29	19.83	Extremely sever
-0.11	0.00	0.00	0.06	3.83	0.01	0.95	0.00	0.00	0.06	3.87	0.01	1.02_ 0.00		sevei
0.13														

7. REFERENCE

Abdulkareem, J. H. et al. (2017) 'Prediction of spatial soil loss impacted by long-term land-use/land-cover change in a tropical watershed', Geoscience Frontiers journal, XXX, pp. 1–15.

Adekalu, K. O., Okunade, D. A. and Osunbitan, J. A. (2006) 'Compaction and mulching effects on soil loss and runoff from two southwestern Nigeria agricultural soils', Geoderma, 137, pp. 226–230.

Al-Abadi, A. M., Al-Temmeme, A. A. and Al-Ghanimy, M. A. (2016) 'A GIS-based combining of frequency ratio and index of entropy approaches for mapping groundwater availability zones at Badra–Al Al-Gharbi–Teeb areas, Iraq', Water Resour. Manag., 2:265–283. doi: 10.1007/s40899-016-0056-5.

Al-Bahrani, H., Abbas, Z., & AL-Yaseri, I. (2021). Environmental Assessment of Groundwater in Najaf Governorate (Iraq) for Irrigation Purposes. Kufa Journal of Engineering, 11(4), 46–57. https://doi.org/10.30572/2018/kje/110404

Al-doski, J. (2013) 'NDVI Differencing and Post-classification to Detect Vegetation Changes in Halabja City, Iraq', IOSR Journal of Applied Geology and Geophysics, pp. 01–10. doi: 10.9790/0990-0120110.

Cakir, H. I., Khorram, S. and Nelson, S. A. C. (2006) 'Correspondence analysis for detecting land cover change', Remote Sensing of Environment, pp. 306–317. doi: 10.1016/j.rse.2006.02.023.

Cheng, J., Zhang, X., Jia, M., Su, Q., Kong, D., & Zhang, Y. (2024). Integrated Use of GIS and USLE Models for LULC Change Analysis and Soil Erosion Risk Assessment in the Hulan River Basin, Northeastern China. Water, 16(241), 1–15.

Defries, R. S. and Townshend, J. R. G. (1994) 'NDVI-derived land cover classifications at a global scale', International Journal of Remote Sensing, 15(17), pp. 3567–3586. doi: 10.1080/01431169408954345.

Durigon, V. L. et al. (2014) 'NDVI time series for monitoring RUSLE cover management factor in a tropical watershed', International Journal of Remote Sensing, 35(2), pp. 441–453. doi: DOI: 10.1080/01431161.2013.871081.

El Baroudy, A. A. (2011) 'Monitoring land degradation using remote sensing and gis techniques in an area of the middle Nile Delta, Egypt', Catena, pp. 201–208. doi: 10.1016/j.catena.2011.05.023.

Fenjiro, I., Zouagui, A. and Manaouch, M. (2020) 'Assessment of Soil Erosion by RUSLE Model using Remote Sensing and GIS - A case study of Ziz Upper Basin Southeast Morocco', Forum geografic. Studii și cercetări de geografie și protecția mediului Volume, XIX(2), pp. 131–142.

Garrigues, S., Allard, D. and Baret, F. (2007) 'Using First- and Second-Order Variograms for Characterizing Landscape Spatial Structures From Remote Sensing Imagery', IEEE TRANSACTIONS ON GEOSCIENCE AND REMOTE SENSING, 45(6), pp. 1823–1837. doi: 10.1109/TGRS.2007.894572.

Gong, W. et al. (2022) 'Estimating the Soil Erosion Response to Land-Use Land-Cover', Water, pp. 1–17.

https://doi.org/https://doi.org/10.3390/w16020241

Ichii, K., Kawabata, A. And Yamaguchi, Y. (2002) 'Global correlation analysis for NDVI and climatic variables and NDVI trends: 1982–1990', Internationa 1 Journal of Remote Sensing, 23(18), pp. 3873–3878. doi: 10.1080/01431160110119416.

Im, J. et al. (2012) 'Vegetation cover analysis of hazardous waste sites in utah and arizona using hyperspectral remote sensing', Remote Sensing, pp. 327–353. doi: 10.3390/rs4020327.

Kebede, Y. S. et al. (2021) 'Modeling soil erosion using RUSLE and GIS at watershed level in the upper beles, Ethiopia', Environmental Challenges 2, (100009 Contents).

Knijff, J. M. van der, Jones, R. J. A. and Montanarella, L. (2002) Soil Erosion Risk Assessment in Italy.

Li, Y. et al. (2005) 'Study on land cover change detection method based on NDVI time series batasets: Change detection indexes design', IEEE, 0-7803–905. doi: 10.1109/IGARSS.2005.1525440 ·

LU, D. et al. (2005) 'Land-cover binary change detection methods for use in the moist tropical region of the Amazon: a comparative study', International Journal of Remote Sensing, 26(1), pp. 101–114.

Lü, Y. et al. (2012) 'A policy-driven large scale ecological restoration: Quantifying ecosystem services changes in the loess plateau of China', PLoS ONE. doi: 10.1371/journal.pone.0031782.

Meusburger, K., Bänninger, D. and Alewell, C. (2010) 'Estimating vegetation parameter for soil erosion assessment in an alpine catchment by means of QuickBird imagery', International Journal of Applied Earth Observation and Geoinformation, pp. 201–207. doi: 10.1016/j.jag.2010.02.009.

Morgan, R. P. C. (2005) Soil erosion and conservation. Third edit, Soil erosion and conservation. Third edit. Blackwell Publishing company.

Nourizadeh, M., Naghavi, H., & Omidvar, E. (2023). The effect of land use and land cover changes on soil erosion in semi-arid areas using cloud-based google earth engine platform and GIS-based RUSLE model. Natural Hazards. https://doi.org/https://doi.org/10.1007/s11069-023-06375-2

Oñate-Valdivieso, F. and Sendra, J. B. (2010) 'Application of GIS and remote sensing techniques in generation of land use scenarios for hydrological modeling', Journal of Hydrology, 395, pp. 256–263. doi: 10.1016/j.jhydrol.2010.10.033.

Panagos, P. et al. (2015) 'Estimating the soil erosion cover-management factor at the European scale', Land Use Policy, 48, pp. 38–50.

Qian, K. et al. (2022) 'Effects of Vegetation Change on Soil Erosion by Water in Major Basins, Central Asia', Remote Sensing. doi: 10.3390/rs14215507.

Renard et al., (1997) Predicting Soil Erosion by Water: A Guide to Conservation Planning with the Revised Universal Soil Loss Equation (RUSLE).

Richards, J. A. (2022) Remote Sensing Digital Image Analysis. 6th editio. Cham, Switzerland: Springer Nature Switzerland AG. doi: 10.1007/978-3-030-82327-6.

Salih, M. A., & Dhiaa, A. H. (2023). Performance Evaluation of the Reverse Osmosis Pilot Plant: Using Sodium Chloride and Magnesium Chloride. Kufa Journal of Engineering, 14(2), 1–11. https://doi.org/10.30572/2018/KJE/140201

Sellers, P. J. (1985) 'Canopy reflectance, photosynthesis and transpiration', International Journal of Remote Sensing, pp. 1335–1372. doi: 10.1080/01431168508948283.

Singh, A. (1989) 'Review Article Digital change detection techniques using remotely-sensed data', International Journal of Remote Sensing, 10(6), pp. 989–1003. doi: 10.1080/01431168908903939.

Spanner, M. A. et al. (1990) 'Remote sensing of temperate coniferous forest leaf area index the influence of canopy closure, understory vegetation and background reflectance', International Journal of Remote Sensing, 11(1), pp. 95–111. doi: 10.1080/01431169008955002.

Tucker, C. J. (1979) 'Red and photographic infrared linear combinations for monitoring vegetation', Remote Sensing of Environment, pp. 127–150. doi: 10.1016/0034-4257(79)90013-0.

Vatandaşlar, C. and Yavuz, M. (2017) 'Modeling cover management factor of RUSLE using very high-resolution satellite imagery in a semiarid watershed', Environmental Earth Sciences. doi: 10.1007/s12665-017-6388-0.

Wang, J., Rich, P. M. and Price, K. P. (2003) 'Temporal responses of NDVI to precipitation and temperature in the central Great Plains, USA', International Journal of Remote Sensing, 24(11), pp. 2345–2364. doi: DOI: 10.1080/01431160210154812.

Weng, Q. (2002) 'Land use change analysis in the Zhujiang Delta of China using satellite remote sensing, GIS and stochastic modelling', Journal of Environmental Management, 64, pp. 273–284. doi: 10.1006/jema.2001.0509.

Wischmeier, W. H. and Smith, D. D. (1978) Predicting Rainfall Erosion Losses A Guide To Conservation Planning, Supplement to Agriculture Handbook No. 537, USDA, Washington.

Wu, Q. et al. (2006) 'Monitoring and predicting land use change in Beijing using remote sensing and GIS', Landscape and Urban Planning, pp. 322–333. doi: 10.1016/j.landurbplan.2005.10.002.

Xiong, M., Leng, G., & Tang, Q. (2023). Global Analysis of the Cover-Management Factor for Soil Erosion Modeling. Remote Sensing, 15(2868), 1–20.

Yun-hao, C., Xiao-bing, L. and Feng, X. (2001) 'NDVI changes in China between 1989 and 1999 using change vector analysis based on time series data', Journal of Geographical Sciences, pp. 383–392. doi: 10.1007/bf02837965.

Zhongming, W. et al. (2010) 'Stratified vegetation cover index: A new way to assess vegetation impact on soil erosion', Catena, 83, pp. 87–93. doi: 10.1016/j.catena.2010.07.006.